Independent Phase and Amplitude Control of a Laser Beam Using a Single-Phase-Only Spatial Light Modulator

Laser-beam shaping is a rapidly developing field of research driven by both technological improvements of beam-shaping devices and the ever-increasing demands of applications. In high-energy laser chains, efficient beam shaping is successfully achieved in the front ends by passive methods such as beam apodization[1] or intracavity mode shaping;[2] however, these static techniques are unable to correct dynamic laser-beam profiles caused by alignment drifts or thermal problems.

Spatial light modulators (SLM's) are versatile devices that can modulate the polarization or the phase of laser beams at high refresh rates. It has been demonstrated that a SLM can be used to compensate for the thermal phase distortion occurring in high-energy glass amplifiers.[3] Similarly, SLM's have been used in high-energy laser applications, such as intracavity beam shaping[4] or focal-spot control.[5] In all these applications, only the phase-modulation capability of the SLM was used; however, there are numerous applications where phase-only modulation can be achieved differently. For instance, deformable mirrors are more attractive when it comes to wavefront correction of a large, high-energy, laser beam. Their scale and damage threshold allow them to be used within the power amplifier, while SLM's are confined to the front end because of their modest size and low damage threshold. Nevertheless, a corrective device that would address both phase and amplitude simultaneously may be successfully used in high-energy lasers to significantly reduce the alignment procedure time, to improve the amplifier fill factor by injecting a more-adapted beam shape, to reduce the risk of damage in the laser chain by removing hot spots, and to improve the on-target characteristics of the beam by better control of the phase.

Several techniques have been proposed to produce complex modulation of an electromagnetic field with an SLM for encoding computer-generated holograms.[6,7] In both cases, two neighboring pixels with a single-dimension modulation capability are coupled to provide the two degrees of freedom required for independent phase and amplitude modulation. In our work, we use a similar approach, but our requirements differ from that of the hologram generation. First, the number of modulation points across the beam does not need to be high because spatial filtering imposes a low-pass limit on the spatial frequencies allowed in the system. Second, a high-efficiency modulation process is required to minimize passive losses. Lastly, the required amplitude-modulation accuracy should be better than measured shot-to-shot beam fluctuations for the correction to be fully beneficial.

In this article, we propose a new method to modulate both the phase and amplitude of a laser beam, with a single-phase-only SLM using a carrier spatial frequency and a spatial filter. As a result, the local intensity in the beam spatial profile is related to the amplitude of the carrier modulation, while its phase is related to the mean phase of the carrier. In the first part of this article, we show the simple relation between the transmitted intensity and the phase-modulation amplitude, and in the second part, we experimentally verify this scheme and use it to demonstrate beam shaping in a closed-loop configuration.

The principle of the modulation is depicted in Fig. 96.19 for the case of a plane wave. The SLM is used as a phase-only device that applies a one-dimensional phase grating to the electric field. As a consequence, the two-dimensional propagation integral reduces to a one-dimensional one. In such a case, the electric field transmitted—or reflected—through the modulator accumulates a phase ϕ given by

$$E' = E_0 \exp\left[j\phi(x)\right], \tag{1}$$

where E_0 can be complex and ϕ is a periodic square phase modulation, of period Λ, oscillating between the values ϕ_1 and ϕ_2. After propagation through a lens, in an *f-f* configuration and under the Fraunhofer approximation, the electromagnetic field distribution at the focus of the lens is proportional to the Fourier transform of Eq. (1). To calculate the Fourier transform of E', one can consider, for instance, the initial electromagnetic field as a sum of two square waves defined by

$$E_1 = E_0 \sum_n \delta(x - n\Lambda) \otimes \mathrm{rect}_{\Lambda/2}(x) \exp(j\phi_1), \tag{2}$$

$$E_2 = E_0 \sum_n \delta(x - n\Lambda) \otimes \mathrm{rect}_{\Lambda/2}(x - \Lambda/2) \exp(j\phi_2), \tag{3}$$

where δ is the Dirac function and $\otimes$ denotes the convolution product. After some algebra, the electromagnetic field distribution at the focus, given as the sum of the Fourier transforms of E_1 and E_2, can be written as

$$\tilde{E} \propto E_0 \sin c\left(\pi \frac{\Lambda\nu}{2}\right) \cos\left(\frac{\Delta\phi}{2} + \pi \frac{\Lambda\nu}{2}\right) \times \exp\left[j\left(\frac{\phi_1 + \phi_2}{2} - \pi \frac{\Lambda\nu}{2}\right)\right] \sum_n \delta(\nu - n/\Lambda), \tag{4}$$

where n is the spatial frequency, and the Dirac comb function represents the diffraction pattern created by the SLM phase grating. Removing the higher-order terms $(|n| > 0)$ in this diffraction pattern with a spatial filter results in an electric field given by Eq. (5), where the amplitude is determined by the phase difference $\Delta\phi$ and the phase is equal to the average of ϕ_1 and ϕ_2:

$$\tilde{E}(0) \propto E_0 \cos\left(\frac{\Delta\phi}{2}\right) \exp\left(j \frac{\phi_1 + \phi_2}{2}\right). \tag{5}$$

This result is still true for finite beams, provided the amplitude and phase of the initial beam slowly vary with respect to the modulation frequency. If the electromagnetic field spatially varies at higher frequencies, then the imaging system will act as a spatial filter and will modify the spatial distribution of light regardless of the application of a phase modulation on the SLM.

In the experimental setup shown in Fig. 96.20, the light source is a pulsed, 300-Hz laser, the beam of which is up-collimated so that it overfills the SLM area and is linearly polarized. It is reflected off the SLM and then imaged on an 8-bit charge-coupled-device (CCD) camera (Cohu 4910 series) or to a Hartmann–Shack wavefront sensor (Wavefront Sciences CLAS-HP). The camera was used mainly for system alignment and diagnostic or whenever high-spatial-resolution beam amplitude measurement was required. The wavefront sensor was used for simultaneous phase and amplitude measurements. We use a non-pixelated, 256-level, phase-only SLM from Hamamatsu (Model X8267) with a 20 × 20-mm^2 active area, optically addressed by a 768 × 768-pixel liquid crystal display (LCD) screen. Thanks to a slight defocus of the imaging system, a continuous phase modulation can be achieved on the SLM at the expense of a slight reduction in the resolution.

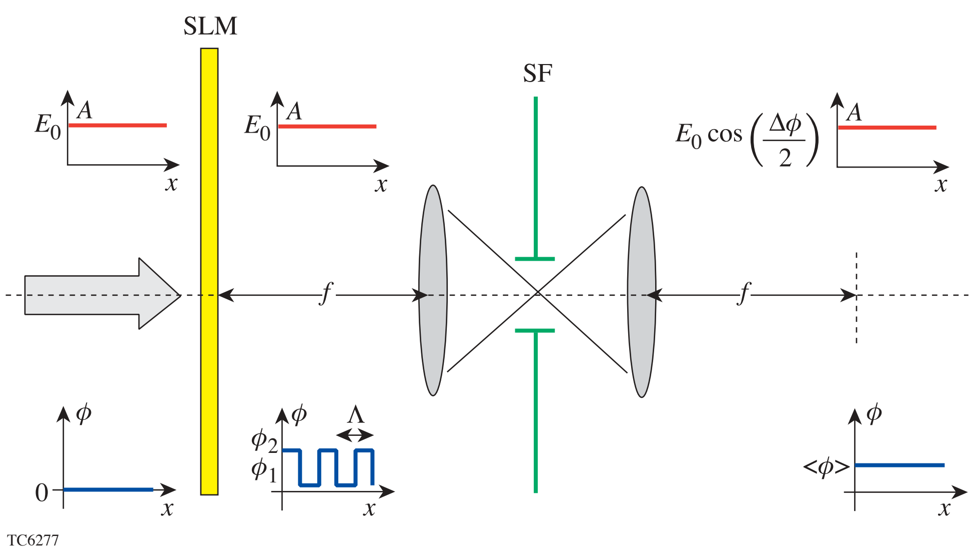

Figure 96.19
Independent phase- and amplitude-modulation scheme. The input beam is modulated in phase by the phase-only SLM and then propagates through a spatial filter (SF). The SLM is placed at a focal distance from the SF lens so the electromagnetic field distribution at the SF pinhole is proportional to the Fourier transform of the electromagnetic field distribution at the SLM location.

Although the SLM was designed for normal-incidence use, we believe that a small angle of incidence does not affect the system's performance. Only a 768×768 matrix is used in the imaging. The advantages of using a non-pixelated SLM are (1) its absence of loss due to the fill factor and diffraction of pixelated SLM and (2) its high damage threshold, which we tested to be 680 ($\pm$130) mJ/cm^2 with a 1-ns, 1053-nm Gaussian beam. This value is nearly two times better than that of the pixelated SLM that we tested.

To be relevant to beam shaping in a high-energy laser facility, such as the OMEGA laser, the pass band of the beam-shaping spatial filter must be at least as large as the spatial filters in the main laser power amplifier, which are as large as 30 times the diffraction limit. To ensure removal of the SLM carrier spatial frequency, the minimum spatial frequency must then be at least 30 times the fundamental spatial frequency of the beam. Practically, this means the minimum number of pixels required for that application is 60 across the beam (two per period). The beam f number in the spatial filter is 25, which means that the diffraction-limited focal spot is roughly 25 μm and the pinhole should be at least 750 μm in diameter. We used a 1-mm pinhole and a modulation frequency 64 times that of the fundamental beam frequency. In the SLM plane, this corresponds to a period of 12 pixels. For lower numbers of pixels per period, the finite slope between two nearby pixels degrades the modulation profile. For larger periods, up to 24 pixels, the beam is efficiently modulated by the SLM, but the system becomes more sensitive to the pinhole alignment.

Figure 96.21 demonstrates a linear amplitude-modulation scheme, as well as high contrast and arbitrary spatial shaping. In the upper part, Eq. (5) is inversed to obtain the phase-modulation amplitude corresponding to a linear amplitude modulation, while the lower part of the image shows nearly complete extinction for a π-rad modulation and ~100% transmission when the phase modulation is 0 rad. The low-contrast speckle, seen in Fig. 96.21, limits the achievable extinction ratio that we measured varying from 50:1 to 10:1 across the beam. It should be noted that the extinction is achieved while only half of the dynamic range of the SLM was used (128 levels), which leaves at least half of the SLM dynamic range free for phase modulation, in the worst case.

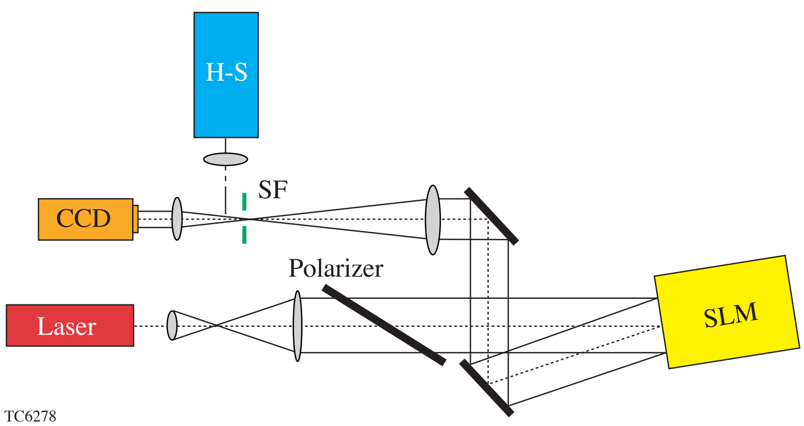

TC6278

Figure 96.20
Experimental setup. SF: spatial-filter pinhole; H–S: Hartmann–Shack wavefront sensor. The SLM is used in reflection and a flip-in mirror is used to measure either the intensity or phase profiles.

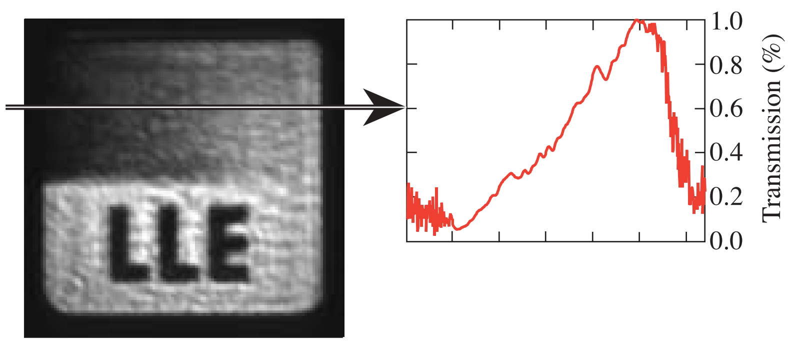

TC6279

Figure 96.21
A modulated beam demonstrates the amplitude control offered by the combined SLM/spatial-filter system. The lineout in the upper portion demonstrates the effective transmission function, while the lower part demonstrates high-contrast modulation with as much as a 50:1 extinction ratio.

Figure 96.22 demonstrates simultaneous amplitude and wavefront-shaping performance of this system by summing two one-dimensional patterns with spatial frequencies below and above the cutoff frequency of the spatial filter, as shown by the mask in Fig. 96.22(a). Figure 96.22(b) shows the beam amplitude measured with the Hartmann–Shack sensor, while Fig. 96.22(c) illustrates the measured wavefront. Both images display data dropout near the center because the measured intensity falls below the detection threshold of the wavefront sensor. Little phase-to-amplitude coupling is observed, demonstrating that the phase information is conserved through the filter while the intensity modulation is achieved.

Figure 96.23 illustrates the performance of this beam-shaping scheme in an iterative, closed-loop configuration. A single convergence scheme is applied in which less amplitude modulation is applied where not enough transmission is achieved and more where too much is measured. For demonstration purposes, we propose to correct the pixels for which the measured intensity on a 8-bit gray scale is higher than 80 counts. After mapping the SLM to the CCD using a fiducial image, the required transmission at each location of the SLM and the corresponding phase-modulation amplitude are calculated. The first step correction result is shown by the image in Fig. 96.23(b) along with its corresponding lineout, which

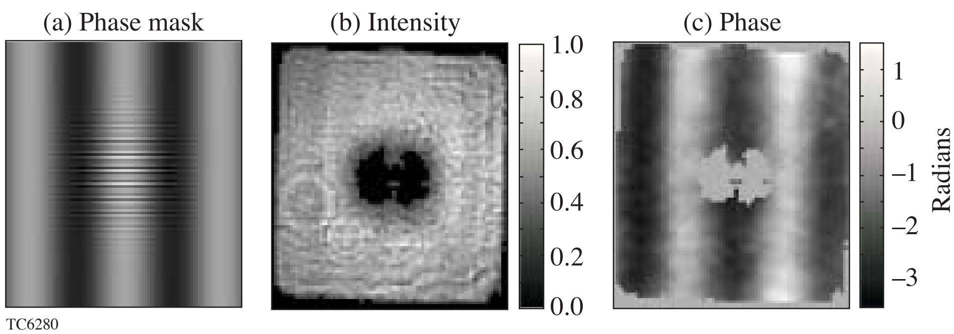

Figure 96.22
Independent phase and amplitude modulation is demonstrated. The mask (a) leads to a beam that exhibits simultaneous amplitude (b) and phase (c) modulation.

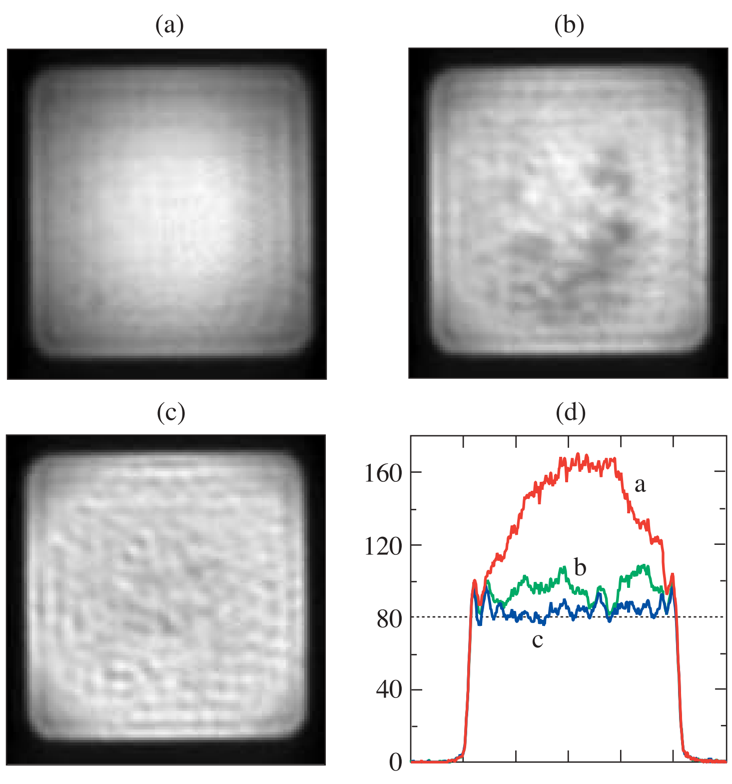

Figure 96.23
Dynamic amplitude beam control. The initial beam (a) is shaped into top-hat beams (b) and (c). The lineouts show the typical error to the intensity goal.

shows that most of the correction factor has been underestimated since the average intensity is above 80 counts. Similarly, the correction does not lead to a uniform beam because of the spatially dependent transfer function of the SLM. Nevertheless, the error, defined as the difference between the real intensity and the goal intensity, in an rms sense, for those points initially higher than 80, is reduced from 60% to 16%. Using image (b), the error signal is reduced by changing the modulation to achieve the goal. The result of a second correction is shown in Fig. 96.23(c), where the error signal has been reduced to 8.5%, which is dominated by the speckle noise discussed earlier.

We have shown a dynamic modulation scheme that addresses simultaneously both the phase and the amplitude of a laser beam. By modulating the phase of a laser beam at high spatial frequencies, one can couple the phase-modulation amplitude to the transmission of a spatial filter in a straightforward way. Following that, we have demonstrated that this scheme can be used for beam correction.

ACKNOWLEDGMENT

This work was supported by the U.S. Department of Energy Office of Inertial Confinement Fusion under Cooperative Agreement No. DE-FC03-92SF19460, the University of Rochester, and the New York State Energy Research and Development Authority. The support of DOE does not constitute an endorsement by DOE of the views expressed in this article.

REFERENCES

1. J. M. Auerbach and V. P. Karpenko, Appl. Opt. **33**, 3179 (1994).
2. V. Bagnoud, J. Luce, L. Videau, and A. Rouyer, Opt. Lett. **26**, 337 (2001).
3. B. Wattellier *et al*., in *OSA Trends in Optics and Photonics (TOPS) Vol. 56, Conference on Lasers and Electro-Optics (CLEO 2001)*, Technical Digest, Postconference Edition (Optical Society of America, Washington, DC, 2001), pp. 70–71.
4. J. Bourderionnet *et al*., Opt. Lett. **26**, 1958 (2001).
5. B. Wattellier *et al*., Opt. Lett. **27**, 213 (2002).
6. J. A. Davis, K. O. Valadéz, and D. M. Cottrell, Appl. Opt. **42**, 2003 (2003).
7. P. Birch *et al*., Opt. Lett. **26**, 920 (2001).